

## Covalent Organic Frameworks

## Sophisticated Design of Covalent Organic Frameworks with Controllable Bimetallic Docking for a Cascade Reaction

Wenguang Leng<sup>+, [a]</sup>, Yongsheng Peng<sup>+, [a]</sup>, Jianqiang Zhang<sup>+, [a]</sup>, Hui Lu<sup>+, [a]</sup>, Xiao Feng<sup>+, [b]</sup>, Rile Ge<sup>+, [a]</sup>, Bin Dong<sup>+, [a]</sup>, Bo Wang<sup>+, [b]</sup>, Xiangping Hu<sup>+, [a]</sup> and Yanan Gao<sup>\*, [a]</sup>

**Abstract:** Precise control of the number and position of the catalytic metal ions in heterogeneous catalysts remains a big challenge. Here we synthesized a series of two-dimensional (2D) covalent organic frameworks (COFs) containing two different types of nitrogen ligands, namely imine and bipyridine, with controllable contents. For the first time, the selective coordination of the two nitrogen ligands of the 2D COFs to two different metal complexes, chloro(1,5-cyclooctadiene)rhodium(I) (Rh(COD)Cl) and palladium(II) acetate (Pd(OAc)<sub>2</sub>), has been realized using a programmed synthetic procedure. The bimetallically docked COFs showed excellent catalytic activity in a one-pot addition-oxidation cascade reaction. The high surface area, controllable metal-loading content, and predesigned active sites make them ideal candidates for their use as heterogeneous catalysts in a wide range of chemical reactions.

Covalent organic frameworks (COFs),<sup>[1–4]</sup> an emerging class of crystalline porous polymers that allow the atomically precise integration of building blocks into periodic networks, have received much attention in catalysis,<sup>[5–12]</sup> gas storage/separation,<sup>[13–17]</sup> sensing,<sup>[18,19]</sup> and energy conversion.<sup>[20–27]</sup> The flexible regulation of the pore parameters (e.g., size, shape, volume, and distribution) and easy introduction of functional active sites to the skeleton of the COFs make them promising platforms for the immobilization of catalysts in organic synthesis. In particular, two-dimensional (2D) COFs possess eclipsed or staggered columnar arrays with one-dimensional (1D) open channels, which not only significantly enhance the diffusion of substances, but can also be used to dock catalysts through the modification of the building blocks of COFs.<sup>[6,28]</sup>

The strong coordination between the organic ligands and metal ions is a general method to introduce metal active sites in catalysts. Given that ligands can be uniformly distributed throughout COFs, their one-to-one interaction with catalysts allows for the effective isolation of the active sites of the catalyst at a molecular level.<sup>[29]</sup> Furthermore, various ligands with different contents and functions can also be introduced into the skeleton of the COFs through sophisticated design. Evidently, these features are not easy to achieve with conventional porous supports. With this in mind, we have developed a novel procedure allowing for the precisely controlled placement of two nitrogen ligands, imine (4,4',4'',4'''-(pyrene-1,3,6,8-tetra-yl)tetraaniline (PyTTA)) and bipyridine (2,2'-bipyridyl-5,5-dialdehyde (2,2'-BPyDCA)), within 2D COFs (Figure 1 a) using a three-component condensation system.<sup>[30]</sup> Four different types of 2D imine-linked COFs were fabricated and named as X% BPy COF (X = 25, 50, 75, 100), in which X% represents the molar percentage of 2,2'-BPyDCA present in the dialdehyde blends. In this way, although the density of the imine groups across the series of 2D COFs remained constant, the number of bipyridine moieties on the channel walls could be varied according to the feeding ratio of the 2,2'-BPyDCA monomer. As such, the selective coordination of the two nitrogen ligands to two different metal complexes, chloro(1,5-cyclooctadiene)rhodium(I) (Rh(COD)Cl) and palladium(II) acetate (Pd(OAc)<sub>2</sub>), can be realized using a programmed synthetic procedure (Figure 1 b).

Fourier transform infrared (FTIR) spectroscopy provided direct evidence for the formation of imine linkages in X% BPy COFs (Figure S1 in the Supporting Information). Elemental analysis showed that the actual nitrogen contents of the COFs were close to the calculated values (Figure S2). Thermogravimetric analysis (TGA) revealed them to be highly thermostable (Figure S3). The 100% BPy COF exhibited strong powder X-ray diffraction (PXRD) peaks at 3.2°, 4.6°, 6.4°, 9.7°, 12.9° and 23.8°, corresponding to the (110), (020), (220), (330), (440) and (001) facets, respectively.<sup>[28]</sup> The similar PXRD patterns were also observed for the other X% BPy COFs, indicating that they have a similar crystal structure (Figure 1 c). The use of lattice-modeling and Pawley refinement processes led to an eclipsed AA stacking model (Figure S4), suggesting the presence of open channels (Figure 1 d). Nitrogen-adsorption isotherms exhibited reversible type-IV curves for the X% BPy COFs, indicative of a mesoporous character (Figure S5). The pore parameters ( $S_{\text{BET}}$  volume, size distribution, and interlayer distance) are summarized in Table 1. The high surface area, good thermostability,

[a] Dr. W. Leng,<sup>+</sup> Y. Peng,<sup>+</sup> J. Zhang, Dr. H. Lu, Dr. R. Ge, Dr. B. Dong, Prof. X. Hu, Prof. Y. Gao

Dalian National Laboratory for Clean Energy  
Dalian Institute of Chemical Physics, Chinese Academy of Sciences  
457 Zhongshan Road, Dalian 116023 (P.R. China)  
E-mail: ygao@dicp.ac.cn

[b] Dr. X. Feng, Prof. B. Wang  
Key Laboratory of Cluster Science, Ministry of Education of China  
School of Chemistry, Beijing Institute of Technology  
5 South Zhongguancun Street, Beijing 100081 (P.R. China)

[†] These authors contributed equally to this work.

Supporting information for this article can be found under <http://dx.doi.org/10.1002/chem.201601334>.

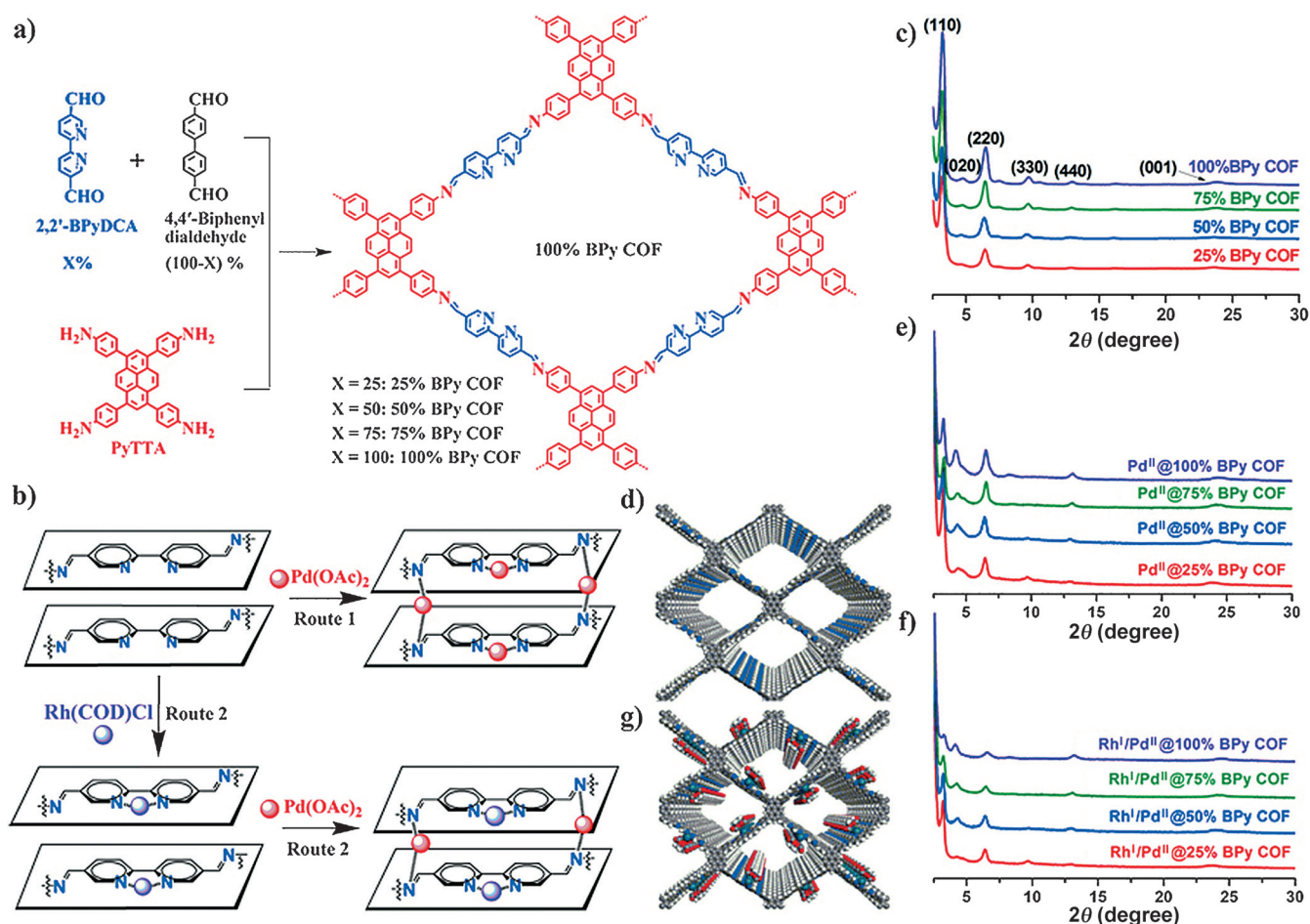


**Figure 1.** a) Use of a three-component condensation system to modulate the nitrogen content of the 2D imine-type COFs. b) Designed strategies for the monometallic (Route 1) and bimetallic docking (Route 2). c) PXRD patterns of the X% BPy COFs. d) Open channels of the COFs. e) PXRD patterns of the Pd@X% BPy COFs. f) PXRD patterns of the Rh/Pd@X% BPy COFs. g) Open channels of the metal loaded COFs.

COFs	$S_{\text{BET}}$ [m <sup>2</sup> g <sup>-1</sup> ]	Pore size [nm]	Pore volume [cm <sup>3</sup> g <sup>-1</sup> ]	Interlayer distance [Å] <sup>[a,b]</sup>
25% BPy COF	538	2.7	0.53	3.77
50% BPy COF	1554	2.6	1.26	3.76
75% BPy COF	1438	2.7	1.11	3.74
100% BPy COF	1288	2.6	0.98	3.73
Pd@25% BPy COF	283	2.3	0.30	3.71
Pd@50% BPy COF	982	2.2	0.59	3.70
Pd@75% BPy COF	847	2.1	0.53	3.68
Pd@100% BPy COF	731	2.0	0.45	3.65
Rh/Pd@25% BPy COF	115	2.4	0.23	3.74
Rh/Pd@50% BPy COF	146	2.4	0.26	3.71
Rh/Pd@75% BPy COF	97	2.4	0.19	3.68

[a] Calculated by the Bragg equation from the PXRD data in Figure S9.  
[b] Interlayer distance of the (001) facet.

and the single type of mesopores revealed that the COFs could be used as catalysts or catalyst carriers.

As a preliminary investigation for the bimetallic docking, monometallic Pd(OAc)<sub>2</sub> was first loaded into the X% BPy COFs

(Figure 1b Route 1) by using a simple solution-infiltration method,<sup>[5,6]</sup> and the resulting composites shall be referred to, hereafter, as Pd@X% BPy COFs. PXRD (Figure 1e) and FTIR spectroscopy (Figure S6) analysis revealed that the structural frameworks of the COFs had been well maintained, while the evident darkening in the color of the solids indicated the successful loading of Pd(OAc)<sub>2</sub> (Figure S7). X-ray photoelectron spectroscopy (XPS) was performed to determine the docking position of the Pd(OAc)<sub>2</sub> (Figure 2a). Bipyridine-free 0% BPy COF<sup>[31]</sup> exhibited a N 1s signal at 398.8 eV, which shifted to 399.2 eV after loading with Pd(OAc)<sub>2</sub>, revealing that Pd(OAc)<sub>2</sub> coordinated to the imine groups.<sup>[32]</sup> The coordination between the bipyridine monomers and Pd(OAc)<sub>2</sub> gave a signal at 400.4 eV. In comparison, a broad peak overlapping both signals at 399.2 eV and 400.4 eV can be seen for all Pd@X% BPy COFs (X = 25, 50, 75, 100), and the intensity of the peak at 400.4 eV increased with increasing 2,2'-BPyDCA content. This result proves that both nitrogen ligands participate in the coordination with Pd(OAc)<sub>2</sub>. We also designed and prepared another bipyridine-free 2D imine-type COF (TF-BD COF, from benzidine (BD) and 1,3,6,8-tetrakis(4-formylphenyl)pyrene (TFPPy)) that could be regarded as the analogue of the

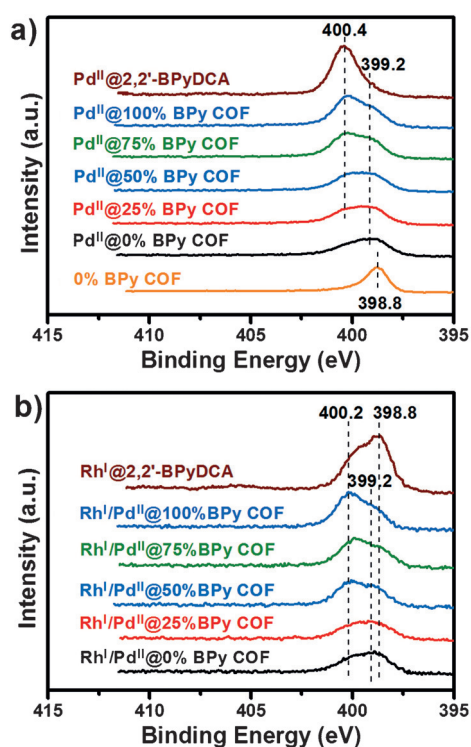


**Figure 2.** XPS results (N 1s) for the different samples before and after docking with a) Pd(OAc)<sub>2</sub> and successive docking with b) Rh(COD)Cl and Pd(OAc)<sub>2</sub>.

0% BPy COF, as both have a similar structure, but with a higher degree of crystallinity of the 0% BPy COF (Figure S8). The Brunauer–Emmett–Teller (BET) surface area and the pore diameter of the *X*% BPy COFs (*X* = 25, 50, 75 and 100) both decreased after loading with Pd(OAc)<sub>2</sub> (Table 1). In contrast, the TF-BD COF showed negligible changes in the pore size before and after the docking of Pd(OAc)<sub>2</sub> (Figure S8). This result indicated that the Pd(OAc)<sub>2</sub> molecules coordinate to the imine groups that are located between adjacent COF sheets, which could not have an influence on the pore diameter.<sup>[5]</sup> Instead, these resided Pd(OAc)<sub>2</sub> molecules pulled the interlayer distance of adjacent COF sheets closer (Table 1), since the PXRD peak assigned to the (001) facet gradually shifted to higher angles (Figure S9a and b). In contrast, coordination of Pd(OAc)<sub>2</sub> to the bipyridine groups could occupy the pore space, and therefore lead to a reduction in the pore size.<sup>[28]</sup> The measured Pd-loading contents were lower than the theoretical maximum values (Figure S10), revealing that the structural regularity of the COF scaffolds was likely to have an impact on the accommodation of Pd(OAc)<sub>2</sub>.

To realize the bimetallic loading, we used a programmed synthetic procedure (Figure 1 b, Route 2). Rh(COD)Cl (7.4 × 6.6 × 5.3 Å)<sup>[33]</sup> is bulky and more rigid than Pd(OAc)<sub>2</sub> (10.6 × 5.0 × 4.3 Å),<sup>[33]</sup> but could still be readily immobilized by the bipyridine units.<sup>[34]</sup> However, it is difficult for Rh(COD)Cl to enter the space between adjacent COFs sheets (the interlayer distance is about 3.74 Å, as measured by PXRD or calculated by simulation). To this end, the docking of Rh(COD)Cl was carried out first and the resulting samples were named as

Rh<sup>I</sup>@*X*% BPy COFs. No evident color change was observed for either 0% BPy COF or TF-BD COF when the samples were loaded with Rh(COD)Cl. Inductively coupled plasma optical emission spectroscopy (ICP-OES) measurements also suggested a negligible Rh content in the two COFs. These results revealed that the large and rigid Rh(COD)Cl molecules did not fit into the space between adjacent COFs sheets. However, for the Rh<sup>I</sup>@*X*% BPy COFs (*X* = 25, 50, 75, 100) a darkening in the color was observed, which indicated the successful loading of Rh(COD)Cl within the COFs (Figure S11). PXRD and FTIR spectroscopy analysis revealed that the structural frameworks of the COFs had been well maintained (Figure S12). The theoretical maximum Rh-loading content of the *X*% BPy COFs, calculated based on the amount of bipyridine, was 5.0, 8.9, 12.0, and 14.6 wt% for *X* values of 25, 50, 75, and 100, respectively. However, the measured values by ICP-OES were lower than those determined theoretically (4.9, 7.8, 7.5, and 7.9 wt%, correspondingly). It is evident that when the molar percentage of 2,2'-BPyDCA is 25%, the Rh-loading content (4.9 wt%) is close to the theoretical value (5.0 wt%), whereas the measured values remain almost unchanged when *X* is increased to 50, 75, and 100%. Considering that the Rh(COD)Cl molecule is large and rigid, it can be assumed that the docking of Rh(COD)Cl reaches its saturation when the molar percentage of 2,2'-BPyDCA is 50%.

The subsequent loading of Pd(OAc)<sub>2</sub> was carried out and the resulting samples were named as Rh<sup>I</sup>/Pd<sup>II</sup>@*X*% BPy COFs. PXRD (Figure 1 f) and FTIR spectroscopy (Figure S13) results revealed that the skeleton of the COFs remained intact, while the color of the materials became further darker in appearance (Figure S14) indicating the successful bimetallic loading. XPS analysis was performed for the different samples after successive Rh(COD)Cl and Pd(OAc)<sub>2</sub> treatments (Figure 2 b). Bipyridine-free Rh<sup>I</sup>/Pd<sup>II</sup>@0% BPy COF exhibited a similar N 1s peak compared to that of Pd<sup>II</sup>@0% BPy COF, further confirming that Rh(COD)Cl could hardly enter the void space between adjacent COF layers. The signal at 398.8 eV was attributed to the coordination between Rh(COD)Cl and bipyridine. This signal could also be seen in the Rh<sup>I</sup>/Pd<sup>II</sup>@*X*% BPy COFs (*X* = 25, 50, 75, 100), confirming that Rh<sup>I</sup> mainly interacted with the bipyridine units. When the bipyridine ratio was low (*X* = 25), the peak at 399.2 eV indicated that Pd(OAc)<sub>2</sub> mainly coordinated with imine groups. However, as the bipyridine ratio increased, the peak at 400.2 eV was gradually intensified. This suggests that a proportion of the bipyridine sites could not be occupied by Rh(COD)Cl due to steric limitations, and the smaller and more flexible Pd(OAc)<sub>2</sub> had a better chance of being immobilized by the residual bipyridine units.

The BET surface areas of the Rh<sup>I</sup>/Pd<sup>II</sup>@*X*% BPy COFs were much lower than those of the Pd<sup>II</sup>@*X*% BPy COFs (Figure S15 and Table 1), again indicating the successful bimetallic loading. The pore diameters of all the Rh<sup>I</sup>/Pd<sup>II</sup>@*X*% BPy COFs were measured to be 2.4 nm (Figure S16). This value is lower than those of their parent *X*% BPy COFs (2.6 or 2.7 nm) but higher than that of the Pd<sup>II</sup>@*X*% BPy COFs (2.3, 2.2, 2.1, and 2.0 nm with *X* values of 25, 50, 75, and 100, respectively). The Rh-loading contents of the Rh<sup>I</sup>/Pd<sup>II</sup>@*X*% BPy COFs were measured to be 4.8,

7.1, 6.1 and 7.7 wt% with  $X$  values of 25, 50, 75 and 100, respectively, which is close to those of the  $\text{Rh}^I@X\%$  BPy COFs (4.9, 7.8, 7.5, 7.9 wt% with  $X$  values of 25, 50, 75 and 100, respectively), suggesting that Rh was apparently not lost after the  $\text{Pd}(\text{OAc})_2$  loading. The Pd-loading contents of the  $\text{Rh}^I/\text{Pd}^{II}@X\%$  BPy COFs were determined to be 8.5, 9.1, 8.0 and 10.7 wt% with  $X$  values of 25, 50, 75 and 100, respectively, which is close to that of bipyridine-free  $\text{Pd}^{II}@0\%$  BPy COF (11.1 wt%), but much lower than that of the  $\text{Pd}^{II}@X\%$  BPy COFs (14.3, 18.2, 18.7 and 16.4 wt% with  $X$  values of 25, 50, 75 and 100, respectively). These results further indicate that  $\text{Pd}(\text{OAc})_2$  molecules mainly occupy the imine sites in the space between adjacent COF layers. The PXRD patterns reveal that after loading with  $\text{Rh}^I$ , the peak assigned to the (001) facet was evidently not shifted compared to their corresponding  $X\%$  BPy COFs (Figure S9c), consistent with the argument that  $\text{Rh}(\text{COD})\text{Cl}$  mainly coordinated with bipyridine units. In contrast, evident shifting of this peak was observed after subsequent  $\text{Pd}^{II}$  docking (Figure S9d), which again supports the assumption that the later added  $\text{Pd}(\text{OAc})_2$  mainly coordinated to the imine groups and pulled the COF layers closer. To sum up, the selective coordination of bipyridine and imine ligands to the metal complexes  $\text{Rh}(\text{COD})\text{Cl}$  and  $\text{Pd}(\text{OAc})_2$  has been realized using the described programmed synthetic procedure (Figure 1 g).

To characterize the catalytic performance of the COFs, the bimetallic  $\text{Rh}^I/\text{Pd}^{II}@X\%$  BPy COFs were used as catalysts for a cascade reaction. As reported by Sakai et al.,<sup>[35]</sup> the  $\text{Rh}^I$ -catalyzed addition of phenylboronic acid to benzaldehyde can produce diphenylmethanol in high yield. On the other hand, diphenylmethanol can be further oxidized to generate benzophenone under  $\text{Pd}^{II}$  catalysis.<sup>[36]</sup> As a result, it is anticipated that the separated loading of  $\text{Rh}^I$  and  $\text{Pd}^{II}$  leads to bimetallic catalysts that could be used to catalyze this cascade reaction, as illustrated in Table 2.

As expected, a 90% yield of the final product was realized with the  $\text{Rh}^I/\text{Pd}^{II}@75\%$  BPy COF as a representative catalyst in a one-pot reaction. To illuminate the respective functions of  $\text{Pd}^{II}$  and  $\text{Rh}^I$  in the cascade reaction, COFs only loaded with  $\text{Pd}^{II}$  or  $\text{Rh}^I$  were investigated. We found that the monometallic  $\text{Pd}^{II}@75\%$  BPy COF did not catalyze the addition of phenylboronic acid to benzaldehyde, as no diphenylmethanol was obtained in the separated reaction. On the other hand, the  $\text{Pd}^{II}@75\%$  BPy COF exhibited an excellent catalytic activity in the oxidation of diphenylmethanol to benzophenone with a yield of 99%. Likewise, the monometallic  $\text{Rh}^I@75\%$  BPy COF failed to catalyze the oxidation of diphenylmethanol to benzophenone, but exhibited a high catalytic activity in the addition of phenylboronic acid to benzaldehyde to produce diphenylmethanol with a yield of 88%, which is comparable to homogeneous  $\text{Rh}^I$  catalysts (92%) reported by Sakai et al.<sup>[35]</sup> These results indicate that  $\text{Rh}^I$  catalyzed the addition reaction and  $\text{Pd}^{II}$  catalyzed the oxidation reaction, as expected. The  $\text{Rh}^I/\text{Pd}^{II}@75\%$  BPy COF was recycled by filtration and its outstanding catalytic activity could be maintained (>85% isolated yield) for up to five cycles of the cascade reaction. ICP-OES results also confirmed that only limited leaching of Rh (ca. 3%) and Pd (ca. 5%) could be observed after the 5th reaction cycle.

**Table 2.** One-pot cascade reactions using different homogeneous/heterogeneous catalysts

Catalyst	Yield of addition reaction [%] <sup>[a]</sup>	Yield of oxidation reaction [%] <sup>[b]</sup>	Yield of cascade reaction [%] <sup>[c]</sup>
$\text{Rh}^I/\text{Pd}^{II}@75\%$ BPy COF	90	99	90
$\text{Rh}^I/\text{Pd}^{II}@75\%$ BPy COF 2nd cycle <sup>[d]</sup>	88	99	87
$\text{Rh}^I/\text{Pd}^{II}@75\%$ BPy COF 3rd cycle	–	–	88
$\text{Rh}^I/\text{Pd}^{II}@75\%$ BPy COF 4th cycle	–	–	87
$\text{Rh}^I/\text{Pd}^{II}@75\%$ BPy COF 5th cycle	–	–	85
$\text{Rh}^I@75\%$ BPy COF	88	0	0
$\text{Pd}^{II}@75\%$ BPy COF	0	99	0
$\text{Rh}(\text{COD})\text{Cl} + \text{Pd}(\text{OAc})_2$ <sup>[e]</sup>	–	–	3
$\text{Rh}(\text{COD})\text{Cl} + \text{Pd}(\text{OAc})_2 + \text{bipyridine ligand}$ <sup>[f]</sup>	–	–	99

[a] Phenylboronic acid (2.0 mmol), benzaldehyde (1.0 mmol), potassium carbonate (3.0 mmol), catalyst (containing 0.01 mmol metal), toluene/ $\text{H}_2\text{O}$  (15 mL/5 mL), 120 °C, 24 h,  $\text{N}_2$  protection. [b] Diphenylmethanol (1.0 mmol), potassium carbonate (3.0 mmol), catalyst (containing 0.01 mmol of metal), toluene/ $\text{H}_2\text{O}$  (15 mL/5 mL), ambient air, 100 °C, 12 h. [c] After the addition reaction, the temperature was directly decreased to 100 °C and  $\text{O}_2$  was purged into the reaction system with other experimental parameters being identical to each stepwise reaction. [d] The COF catalyst was filtrated and reused for another round of the cascade catalysis. [e]  $\text{Rh}(\text{COD})\text{Cl}$  (0.01 mmol) and  $\text{Pd}(\text{OAc})_2$  (0.01 mmol) as homogeneous catalyst. [f]  $\text{Rh}(\text{COD})\text{Cl}$  (0.01 mmol),  $\text{Pd}(\text{OAc})_2$  (0.01 mmol), and bipyridine ligand (0.02 mmol) as homogeneous catalyst.

Additionally, the well-preserved crystalline structure of the bimetallic docked COFs also verified their high resistance to the conducted catalytic conditions. The heterogeneous nature of the catalyst was verified by a leaching test. In a typical experiment, the supernatant after one cycle of the catalytic reaction was isolated and mixed with fresh reactants for another cycle of the cascade reaction without the heterogeneous catalyst. As expected, no signal of the target product was observed under such conditions. We also attempted to catalyze the cascade reactions by homogeneous catalysts under identical experimental conditions. In the absence of nitrogen ligands, the combination of  $\text{Rh}(\text{COD})\text{Cl}$  with  $\text{Pd}(\text{OAc})_2$  could hardly catalyze the cascade reaction (only 3% yield). In contrast, the yield reached 99% when both complexes,  $\text{Rh}(\text{COD})\text{Cl}$  and  $\text{Pd}(\text{OAc})_2$ , together with the bipyridine ligand mixture were used as homogeneous catalysts. This result suggests the necessity of the coordination between the metals and the nitrogen ligands to ensure effective catalysis. This, in turn, reveals that the carefully designed

coordination of the two nitrogen ligands to the two different metal complexes in this work is of significance to guarantee both, precise docking of the metal sites and high catalytic activity of the loaded catalysts.

In summary, a series of 2D COFs containing imine and bipyridine ligands with variable contents were synthesized. The selective coordination of the two nitrogen ligands to two different metal complexes, Rh(COD)Cl and Pd(OAc)<sub>2</sub>, can be realized using a programmed synthetic procedure. The larger and rigid Rh(COD)Cl predominantly coordinates with the bipyridine moieties in the pores of COFs, whereas the smaller and flexible Pd(OAc)<sub>2</sub> mainly occupies the remaining imine sites in the space between adjacent COF layers. The bimetallic Rh<sup>I</sup>/Pd<sup>II</sup>-based COF exhibited an excellent catalytic activity in a one-pot addition–oxidation cascade reaction. We believe that such a strategy might be extended to other bimetallic systems (e.g., Rh/Pt, Ir/Pd) in catalyzing other sorts of cascade reactions or even generate synergistic effects to enhance the selectivity or activity of other reactions.

## Acknowledgements

This work was supported by the National Natural Science Foundation of China (21273235, 21473196 and 21403214) and the 100-Talents Program of the Chinese Academy of Sciences.

**Keywords:** cascade reactions · covalent organic frameworks · heterogeneous catalysis · metal loading · nitrogen ligands

- [1] A. P. Côté, A. I. Benin, N. W. Ockwig, M. O’Keeffe, A. J. Matzger, O. M. Yaghi, *Science* **2005**, *310*, 1166–1170.
- [2] H. M. El-Kaderi, J. R. Hunt, J. L. Mendoza-Cortés, A. P. Côté, R. E. Taylor, M. O’Keeffe, O. M. Yaghi, *Science* **2007**, *316*, 268–272.
- [3] X. Feng, X. S. Ding, D. L. Jiang, *Chem. Soc. Rev.* **2012**, *41*, 6010–6022.
- [4] S. Y. Ding, W. Wang, *Chem. Soc. Rev.* **2013**, *42*, 548–568.
- [5] S. Y. Ding, J. Gao, Q. Wang, Y. Zhang, W. G. Song, C. Y. Su, W. Wang, *J. Am. Chem. Soc.* **2011**, *133*, 19816–19822.
- [6] H. Xu, X. Chen, J. Gao, J. B. Lin, M. Addicoat, S. Irle, D. L. Jiang, *Chem. Commun.* **2014**, *50*, 1292–1294.
- [7] P. Pachfule, S. Kandambeth, D. Díaz Díaz, R. Banerjee, *Chem. Commun.* **2014**, *50*, 3169–3172.
- [8] P. Pachfule, M. K. Panda, S. Kandambeth, S. M. Shivaprasad, D. Díaz Díaz, R. Banerjee, *J. Mater. Chem. A* **2014**, *2*, 7944–7952.
- [9] Q. R. Fang, S. Gu, J. Zheng, Z. B. Zhuang, S. L. Qiu, Y. S. Yan, *Angew. Chem. Int. Ed.* **2014**, *53*, 2878–2882; *Angew. Chem.* **2014**, *126*, 2922–2926.
- [10] K. N. Zhang, O. K. Farha, J. T. Hupp, S. T. Nguyen, *ACS Catal.* **2015**, *5*, 4859–4866.
- [11] Y. G. Zhang, J. Y. Ying, *ACS Catal.* **2015**, *5*, 2681–2691.
- [12] Y. G. Zhang, S. N. Riduan, *Chem. Soc. Rev.* **2012**, *41*, 2083–2094.
- [13] S. S. Han, H. Furukawa, O. M. Yaghi, W. A. Goddard III, *J. Am. Chem. Soc.* **2008**, *130*, 11580–11581.
- [14] H. Furukawa, O. M. Yaghi, *J. Am. Chem. Soc.* **2009**, *131*, 8875–8883.
- [15] C. J. Doonan, D. J. Tranchemontagne, T. G. Glover, J. R. Hunt, O. M. Yaghi, *Nat. Chem.* **2010**, *2*, 235–238.
- [16] H. P. Ma, H. Ren, S. Meng, Z. J. Yan, H. Y. Zhao, F. X. Sun, G. S. Zhu, *Chem. Commun.* **2013**, *49*, 9773–9775.
- [17] M. G. Rabbani, A. K. Sekizkardes, Z. Kahveci, T. E. Reich, R. S. Ding, H. M. El-Kaderi, *Chem. Eur. J.* **2013**, *19*, 3324–3328.
- [18] S. Dalapati, S. B. Jin, J. Gao, Y. H. Xu, A. Nagai, D. L. Jiang, *J. Am. Chem. Soc.* **2013**, *135*, 17310–17313.
- [19] J. Zhang, L. B. Wang, N. Li, J. F. Liu, W. Zhang, Z. B. Zhang, N. C. Zhou, X. L. Zhu, *CrystEngComm* **2014**, *16*, 6547–6551.
- [20] S. Wan, J. Guo, J. Kim, H. Ihee, D. L. Jiang, *Angew. Chem. Int. Ed.* **2008**, *47*, 8826–8830; *Angew. Chem.* **2008**, *120*, 8958–8962.
- [21] S. Wan, J. Guo, J. Kim, H. Ihee, D. L. Jiang, *Angew. Chem. Int. Ed.* **2009**, *48*, 5439–5442; *Angew. Chem.* **2009**, *121*, 5547–5550.
- [22] X. Feng, L. Chen, Y. Honsho, O. Saengsawang, L. L. Liu, L. Wang, A. Saeki, S. Irle, S. Seki, Y. P. Dong, D. L. Jiang, *Adv. Mater.* **2012**, *24*, 3026–3031.
- [23] E. L. Spittle, J. W. Colson, F. J. Uribe-Romo, A. R. Woll, M. R. Giovino, A. Saldivar, W. R. Dichtel, *Angew. Chem. Int. Ed.* **2012**, *51*, 2623–2627; *Angew. Chem.* **2012**, *124*, 2677–2681.
- [24] M. Dogru, M. Handloser, F. Auras, T. Kunz, D. Medina, A. Hartschuh, P. Knochel, T. Bein, *Angew. Chem. Int. Ed.* **2013**, *52*, 2920–2924; *Angew. Chem.* **2013**, *125*, 2992–2996.
- [25] L. Chen, K. Furukawa, J. Gao, A. Nagai, T. Nakamura, Y. P. Dong, D. L. Jiang, *J. Am. Chem. Soc.* **2014**, *136*, 9806–9809.
- [26] C. R. DeBlase, K. E. Silberstein, T. T. Truong, H. D. Abruña, W. R. Dichtel, *J. Am. Chem. Soc.* **2013**, *135*, 16821–16824.
- [27] L. Stegbauer, K. Schwinghammer, B. V. Lotsch, *Chem. Sci.* **2014**, *5*, 2789–2793.
- [28] X. Chen, N. Huang, J. Gao, H. Xu, F. Xu, D. L. Jiang, *Chem. Commun.* **2014**, *50*, 6161–6163.
- [29] L. Y. Chen, S. Rangan, J. Li, H. F. Jiang, Y. W. Li, *Green Chem.* **2014**, *16*, 3978–3985.
- [30] A. Nagai, Z. Q. Guo, X. Feng, S. B. Jin, X. Chen, X. S. Ding, D. L. Jiang, *Nat. Commun.* **2011**, *2*, 536.
- [31] This bipyridine-free 2D imine-linked COF product was poorly crystalline with a low surface area (Figure S17). However, it was still synthesized for comparison with the different sorts of X% BPy COFs to illustrate the role of the bipyridine units towards the docking metals.
- [32] A. A. Tregubov, K. Q. Vuong, E. Luais, J. J. Gooding, B. A. Messerle, *J. Am. Chem. Soc.* **2013**, *135*, 16429–16437.
- [33] The molecular size of both Rh(COD)Cl and Pd(OAc)<sub>2</sub> was determined by Material Studio Geometry Optimization by using the CASTED calculation module component built-in the Material Studio software.
- [34] S. K. Goforth, R. C. Walroth, L. McElwee-White, *Inorg. Chem.* **2013**, *52*, 5692–5701.
- [35] M. Sakai, M. Ueda, N. Miyaura, *Angew. Chem. Int. Ed.* **1998**, *37*, 3279–3281; *Angew. Chem.* **1998**, *110*, 3475–3477.
- [36] R. A. Sheldon, *Catal. Today* **2015**, *247*, 4–13.

Received: March 21, 2016

Published online on May 25, 2016